JACS
JOURNAL OF THE AMERICAN CHEMICAL SOCIETY

ARTICLE

pubs.acs.org/JACS

Switchable Supramolecular Polymers from the Self-Assembly of a Small Monomer with Two Orthogonal Binding Interactions

Gerd Gröger,[†] Wolfgang Meyer-Zaika,[‡] Christoph Böttcher,[§] Franziska Gröhn,*[,∥] Christian Ruthard,[⊥] and Carsten Schmuck*[,†]

[†]Institut für Organische Chemie, and [‡]Institut für Anorganische Chemie, Universität Duisburg-Essen, Universitätsstrasse 7, 45141 Essen, Germany

[§]Forschungszentrum für Elektronenmikroskopie, Institut für Chemie und Biochemie, Freie Universität Berlin, 14195 Berlin, Germany

[∥]Department of Chemistry and Pharmacy, Interdisciplinary Center for Molecular Materials (ICMM), Friedrich-Alexander-Universität Erlangen-Nürnberg, Egerlandstrasse 3, D-91058 Erlangen, Germany

[⊥]Max Planck Institute for Polymer Research, Ackermannweg 10, D- 55128 Mainz, Germany

Supporting Information

ABSTRACT: The low molecular weight heteroditopic monomer **1** forms supramolecular polymers in polar solution as shown, for example, by infrared laser-based dynamic light scattering (DLS), small-angle neutron scattering (SANS), electron microscopy (TEM, cryo-TEM), and viscosity measurements. Self-assembly of **1** is based on two orthogonal binding interactions, the formation of a Fe(II)-terpyridine 1:2 metal−ligand complex and the dimerization of a self-complementary guanidiniocarbonyl pyrrole carboxylate zwitterion. Both binding interactions have a sufficient stability in polar (DMSO) and even aqueous solutions to ensure formation of linear polymers of considerable length (up to 100 nm). The supramolecular polymerization follows a ring−chain mechanism causing a significant increase in the viscosity of the solutions at millimolar concentrations and above. The linear polymers then further aggregate in solution into larger globular aggregates with a densely packed core and a loose shell. Both binding interactions can be furthermore switched on and off either by adding a competing ligand to remove the metal ion and subsequent readdition of Fe(II) or by reversible protonation and deprotonation of the zwitterion upon addition of acid or base. The self-assembly of **1** can therefore be switched back and forth between four different states, the monomer, a metal-complexed dimer or an ion paired dimer, and finally the polymer.

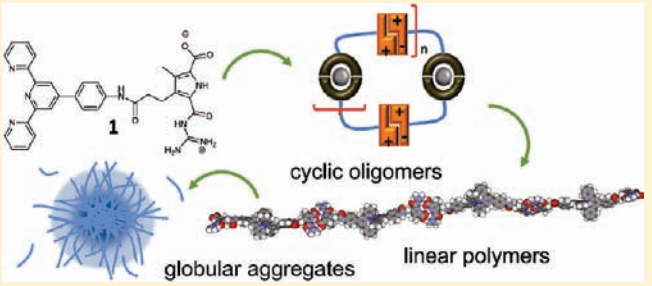

INTRODUCTION

This work describes the reversible formation of linear main-chain supramolecular polymers based on the self-assembly of a small ditopic monomer **1** with two orthogonal binding interactions, metal−ligand binding and ion pair formation. Polymer formation in this case can be reversibly switched on and off by either the addition of acid or base or the addition or removal of metal ions. Supramolecular polymers have become an increasing field of research in the last 20 years as an interesting new class of materials.[1] Besides the functionalization of covalent polymers with supramolecular binding sites, which can be used to further aggregate the macromolecule into even larger structures,[2] so-called main-chain supramolecular polymers are especially interesting.[3] In contrast to traditional covalent polymers, in such systems the individual monomers are held together by noncovalent interactions,[4] and hence the supramolecular interaction is part of the polymer backbone. Therefore, formation of the polymer is reversible (at least under certain conditions) and can be controlled, for example, by changes in concentration, solvent, or temperature or by the addition of external stimuli (e.g., metal ions, protons).[5] Supramolecular polymers not only possess polymer-like properties (e.g., higher viscosity and elasticity), but these properties can also adapt to changes in their surroundings.[6] A fascinating aspect is the possibility of supramolecular polymers to self-heal structural defects because of the reversible nature of the noncovalent interaction between the individual monomers.[7] One challenge in the field is to find suitable small molecular weight monomers, which self-assemble strongly enough in solution to obtain a sufficient degree of polymerization. The degree of polymerization depends on the stability of the noncovalent interaction responsible for polymerization. The first examples of supramolecular polymers as introduced by Lehn[8] or Meijer[9] were based on hydrogen-bonding interactions. Especially the self-complementary ureidopyrimidone quadruple AADD H-bonding motif developed by Meijer has attracted a lot of attention in this respect.[10,11] However, the major disadvantage of purely H-bonded supramolecular

Received: February 9, 2011
Published: May 04, 2011

Scheme 1. Synthesis of the Heteroditopic Monomer 1

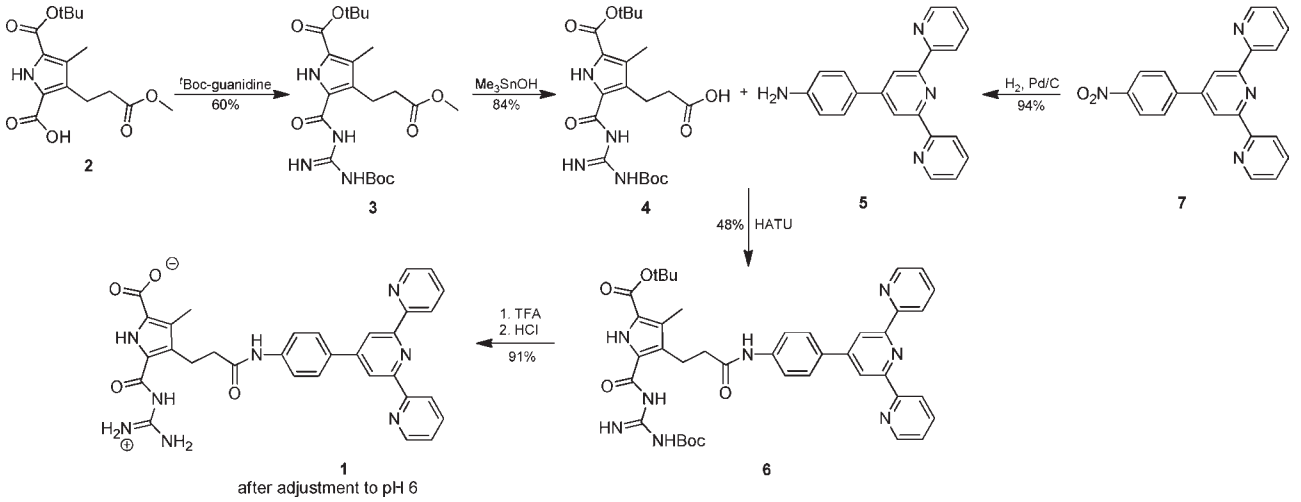

polymers is the weakness of this interaction under competitive polar conditions. Hydrogen bonds are only stable in nonpolar organic solvents such as chloroform but dissociate in more polar and especially protic solvents.[12] Hence, self-assembled systems, which are solely based on this interaction only, are not stable, for example, in aqueous solutions.[13] H-bonds as well as other electrostatic interactions can, however, become more stable within the shielding surrounding of a less polar microenvironment (e.g., hydrophobic pockets within an organic polymer or dendrimer shell).[14,15] More often, additional binding interactions such as Coulomb,[16] hydrophobic, or aromatic stacking interactions[17] are introduced to obtain more stable self-assembled systems in water. Some recent examples are based on amphiphiles with aromatic cores (such as perylenbisimides,[18,19] π-conjugated phenylenes,[20] cyclotriveratrylenes,[21] or hexacorobenzene,[22] just to name a few), functionalized dipolar dyes,[23] cyclodextrins and calixarenes,[24] or macroion−counterion interaction.[25,16b] A special case is metal−ligand interaction, which also has been used extensively to construct supramolecular polymers.[26] As the strength of metal−ligand binding can approach that of covalent bonds, metallo-supramolecular polymers can be nearly as stable as traditional covalent ones and therefore can also reach very large degrees of polymerization.

Most often, supramolecular polymerization is based on one main type of binding site or a set of binding interactions (e.g., H-bonding and π-stacking), which together are responsible for aggregation. For example, a combination of ionic interaction and π-stacking can lead to nonlinear supramolecular polymers with various shapes.[27] However, there are also examples in which two or more binding sites independently, in an orthogonal way, lead to stepwise polymerization.[28] The first example for such a supramolecular polymer with two orthogonal binding sites was introduced by Schubert et al. who functionalized a polyethylene glycol polymer with a self-complementary H-bonding AADD binding site on the one end and a terpyridine ligand on the other end, respectively.[29] In this case, however, the monomer was already a polymer, and due to the use of H-bonds for one binding site supramolecular polymerization was limited to chloroform. Yashima combined metal−ligand binding with much stronger charge interactions instead of H-bonds and presented linear metallo-supramolecular polymers, which are either cationic or anionic due to amidinium or carboxylate groups incorporated into the strands.[30] Hence, two complementary strands form a helical supramolecular heteroduplex held together by ion pairing. Despite these fascinating examples of supramolecular polymers, it is still a challenge to develop new molecules forming stable supramolecular polymers of sufficient length in polar solutions and even more so to be able to deliberately control their formation reversibly by external stimuli.[31] In this respect, we recently introduced a new type of a linear supramolecular polymer in which two orthogonal binding sites are responsible for polymerization within a single strand.[32] We designed the small heteroditopic molecule **1** in which a terpyridine ligand is attached to a self-complementary guanidiniocarbonyl pyrrole carboxylate zwitterion. This zwitterion was developed earlier by us and forms very stable dimers ($K_{ass} > 10^8$ M^{-1} in DMSO) held together by H-bond assisted ion pairs.[33] Addition of a metal ion such as Fe(II) then further polymerized these ion paired dimers into a linear supramolecular polymer. In a preliminary report,[32] we could demonstrate the formation of such linear polymer strands, for example, on solid support by atomic force microscopy (AFM) and in solution using DOSY NMR spectroscopy. We have now studied the self-assembly of **1** in more detail using infrared laser-based dynamic light scattering as well as small-angle neutron scattering (SANS) and electron microscopy (TEM, cryoTEM). We provide evidence for the mechanism of polymer formation and show how polymer formation not only changes the macroscopic properties of the solution (viscosity) but can be reversibly switched on and off by the addition of acid or base and the addition or removal of the metal ions.

RESULTS AND DISCUSSION

Synthesis of Monomer 1. The ditopic monomer **1** was synthesized as shown in Scheme 1. The pyrrole tricarboxylic acid **2** was coupled to N-Boc guanidine using HCTU as coupling reagent. The ester group in the propyl side chain of **3** was then selectively hydrolyzed with trimethyl tinhydroxide to obtain acid **4**, which was reacted with the amine-functionalized terpyridine **5** to give the protected precursor **6**. Ligand **5** is easily accessible from reduction of *p*-nitrophenyl-terpyridine **7**, which can be

dx.doi.org/10.1021/ja200941a |*J. Am. Chem. Soc.* 2011, 133, 8961–8971

Scheme 2. Self-Assembly of a Heteroditopic Monomer 1 Based on Two Orthogonal Binding Interactions, Metal−Ligand Binding and Ion Pair Formation[a]

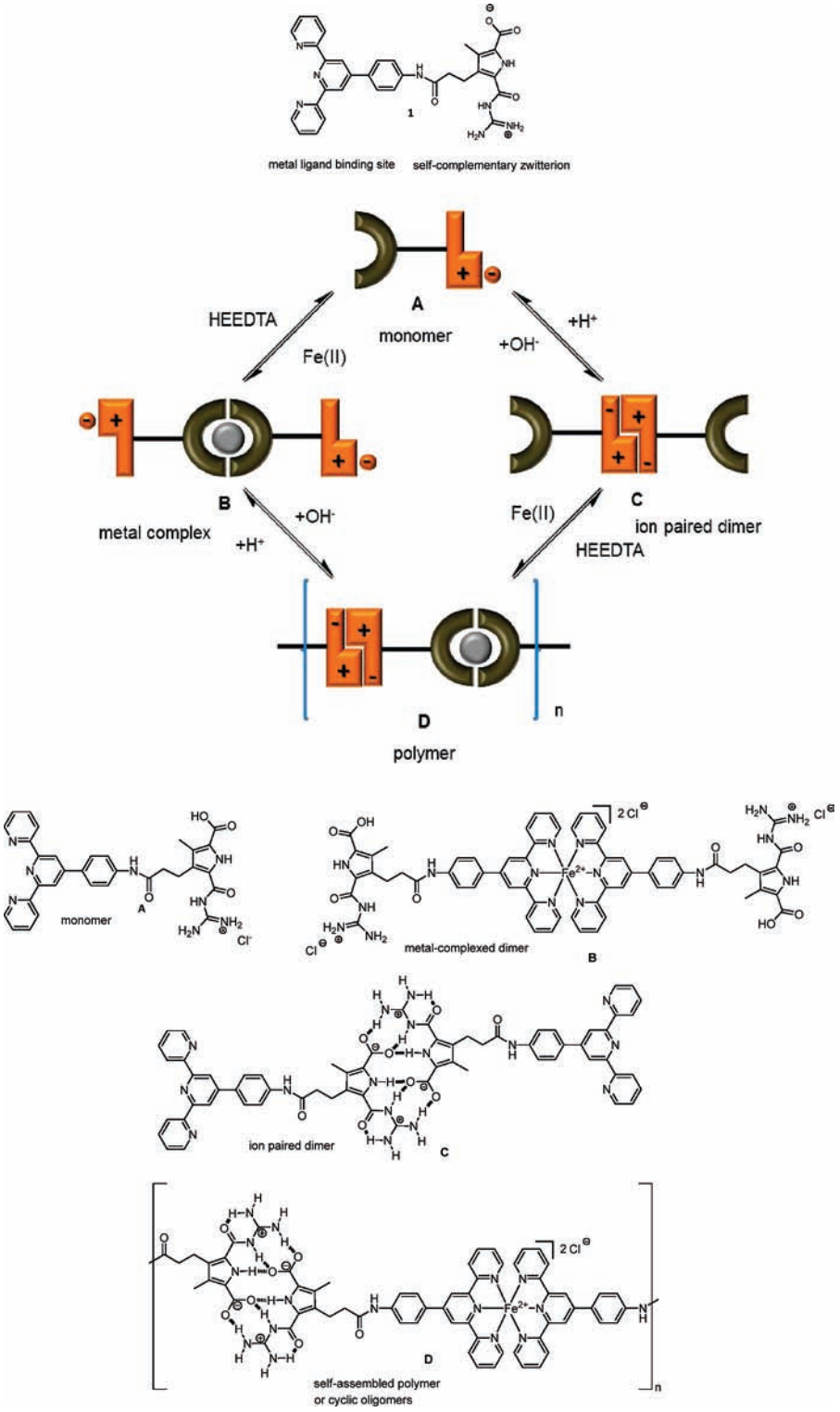

[a] The system can be switched from monomer **A** to either a metal-complexed (**B**) or ion paired dimer (**C**), on to larger self-assembled aggregates **D** (such as cyclic oligomers or linear polymers depending on the concentration of the solution).

synthesized following a literature protocol.[34] After cleavage of the protecting groups in **6** with TFA, the heteroditopic monomer **1** was obtained as a slightly yellow zwitterion after pH adjustment.

Self-Assembly of 1. As shown in Scheme 2, monomer **1** can reversibly change from monomer **A** (e.g., in form of the protonated chloride salt **1•HCl**), to a 2:1 metal complex **B** or an ion

dx.doi.org/10.1021/ja200941a |*J. Am. Chem. Soc.* 2011, 133, 8961–8971

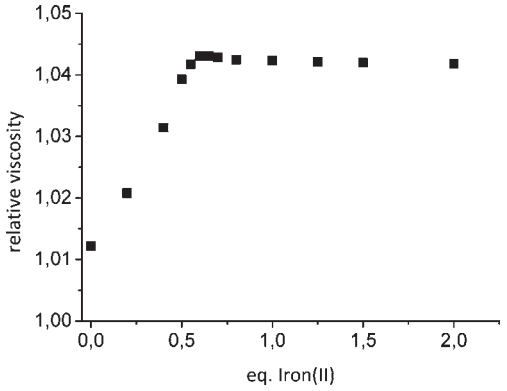

Figure 1. Change of the viscosity of a solution of ion paired dimer **C** (2.5 mM in DMSO) upon the addition of aliquots of Fe(II), confirming the formation of a more viscous polymer **D** due to the formation of a 1:2 metal−ligand complex.

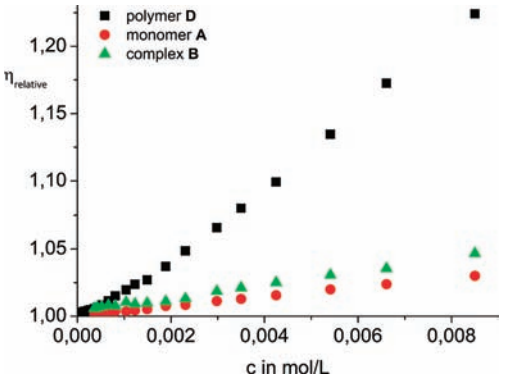

Figure 2. Concentration dependence of the relative viscosity of solutions of polymer **D**, monomer **A** (protonated chloride salt of **1**), and the metal complex **C** in DMSO.

paired dimer **C** and then further on to larger self-assembled aggregates **D** depending on the absence and presence of two chemical stimuli (pH value, Fe(II) ion). Either signal alone only leads to the formation of dimers; only when both signals are present simultaneously can larger aggregates be formed. Because of the pK_a values of the zwitterion (ca. 5 for the carboxylic acid and 7 for the guanidinium cation, respectively), the zwitterion is only present within a pH range from 5 to 7. This pH range allows facile protonation and deprotonation of zwitterion **1** under ambient conditions, thereby eliminating the self-complementarity of this binding site. Neither the protonated cation nor the deprotonated anion can dimerize in polar solution.[35] The metal ion can be removed by the addition of a competing ligand such as HEEDTA (vide infra).

Self-assembly of **1** is therefore a stepwise process, which can be accomplished in two ways. At a pH of 5−7, compound **1** exists as a zwitterion, which in solution self-assembles into the ion paired dimer **C**.[33] Because of the very high stability of this dimer (K_{dim} > 10^8 M^{-1} in DMSO), no monomer can be detected even down to micromolar concentrations (as tested by NMR and UV/vis dilution studies, data not shown). Subsequent addition of 0.5 equiv of iron(II) chloride to a solution of this dimer **C** leads immediately to the appearance of a violet-blue color, indicating formation of the terpyridine−iron(II) 2:1 complex and thus of self-assembled aggregates **D** (self-assembly route **A** → **C** → **D**). Formation of **D** can also be achieved the other way around, starting from the protonated cation of **1**, the monomer **A**, which cannot dimerize, then adding the metal to form the metal-complexed dimer **B** and adjusting the pH afterward to get **D** (self-assembly route **A** → **B** → **D**). The appearance of the violet-blue color is typical for terpyridine−metal complexes and is due to the occurrence of a metal to ligand charge transfer band at λ = 580 nm.[36] A UV/vis titration experiment in which the appearance of this MLCT band was monitored quantitatively upon addition of aliquots of Fe(II) confirmed the formation of the 2:1 complex and provided a stability of K_{ass} > 10^8 M^{-2} under these conditions.[32] All binding steps can also be monitored by characteristic proton shifts in the NMR spectra, which also showed that neither the zwitterionic binding site nor the terpyridine coordination site affect each other.[32] For example, after metal complexation to form **B**, the signals of the terpyridine ligand do not show any further shift change when self-assembly occurs to form **D** upon pH adjustment. Also, the characteristic shifts of the ion paired dimer **C** do not change further, when the metal ion is added and **D** is formed. Hence, the two binding sites are orthogonal; the binding properties of the one site are not affected by the other.

Viscosity Studies. As both interactions, metal−ligand binding and ion pair formation, are very stable, the formation of supramolecular polymers with a significant degree of polymerization even in polar solution was expected. This was first probed using capillary viscosity measurements as the formation of a supramolecular polymer should change the macroscopic properties of the solution.[9,5] The viscosity measurements were performed at 25 °C in DMSO with a Schott visco pump II AVS 370 and a type I micro Ubbelohde capillary. Aliquots of iron(II) chloride (80.0 mM stock solution) were added to a solution of the ion paired dimer **C** (2.5 mM) in DMSO. After the mixture was stirred for 20 min to ensure complete complexation, the relative viscosity was measured (Figure 1). An increase of the viscosity was observed until 0.5 equiv of Fe(II) was added, after which further metal addition did not cause any more changes of the viscosity. This is consistent with the self-assembly of the ion paired dimers **C** present initially in solution into the polymer **D** due to the formation of a 1:2 iron−terpyridine complex (as also seen in the UV/vis titration experiments).

Self-assembly is a concentration-dependent process. Therefore, in contrast to a conventional covalent polymer, also the viscosity of solutions of **1** depends on the concentration as shown again by dilution capillary viscosity experiments in DMSO (T = 30 °C). For example, the relative viscosity for **D** significantly increases to a value of η_{rel} = 1.22 at c = 8.5 mM (Figure 2), which is neither the case for monomer **A** (c = 8.5 mM, η_{rel} = 1.02), nor the 2:1 metal complex **B** (c = 8.5 mM, η_{rel} = 1.04), nor the protected precursor **8** (data not shown).

A closer look at the concentration dependence of the viscosity of polymer **D** allows for gaining further insight into the mechanism of polymer formation.[37] A double-logarithmic plot of the specific viscosity ($\eta_{specific}$) versus the concentration shows two lines with slopes of 0.56 and 1.17, which intersect at a critical polymerization concentration (CPC) of $c \approx 0.35$ mM (Figure 3). The appearance of a CPC is a strong indication for a ring−chain polymerization mechanism.[38] Monomer **1** is flexible enough to form cyclic structures (see also Figure 5) as required for a ring−chain supramolecular polymerization (Figure 4). Furthermore, the intermolecular association constants for both the metal−ligand complexation and the dimerization of the zwitterion are large enough ($K \geq 10^8$ in DMSO) to give rise to the

dx.doi.org/10.1021/ja200941a |*J. Am. Chem. Soc.* 2011, 133, 8961–8971

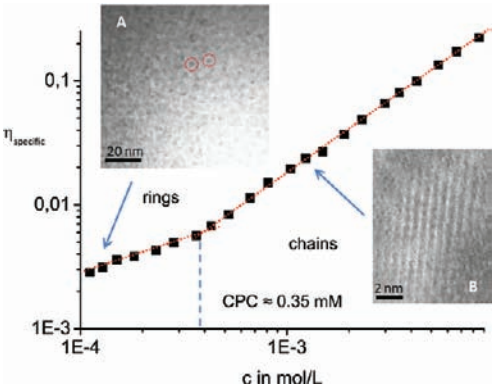

Figure 3. Double-logarithmic plot of the specific viscosity ($\eta_{specific}$) versus the concentration of **D**, suggesting a ring−chain polymerization mechanism. The insets show TEM images recorded below (0.1 mM (A)) and above (1 mM (B)) the CPC, also confirming the predominant formation of cyclic and linear structures under these conditions.

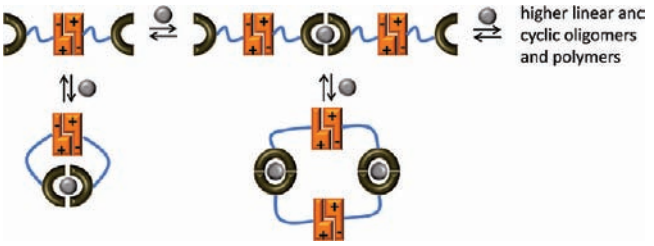

Figure 4. Schematic representation of the ring−chain polymerization mechanism of monomer **1**. The linker between the two binding sites is flexible enough that small cyclic oligomers such as dimers or tetramers can form, which are in equilibrium with linear ones. At low concentrations, the cycles are preferred, whereas with increasing concentrations the equilibrium shifts toward the linear polymers.

occurrence of a critical concentration as pointed out by Ercolani.[37b,38b] At lower concentrations (below CPC), first the formation of cyclic oligomers takes place, and only small changes in the viscosity of the solution are observed. These cyclic oligomers are in equilibrium with linear ones but are favored entropically in dilute solutions. Above the CPC, chain growth at the expense of the cycles becomes more favorable, and the polymerization degree of the linear polymers increases significantly as seen in the steeper slope of the specific viscosity (Figure 3).

Electron Microscopy. Transmission electron microscopy (TEM) confirmed the ring−chain polymerization model deduced from the viscosity data. A drop of a diluted solution of the sample was brought on a holey carbon film coated copper grid. After the excess of solvent was removed with a piece of filter paper and the grid was dried, the grid was stained with an ethanolic solution of uranyl acetate (1% by weight) for 2 min. Excess of staining agent was removed by rinsing with ethanol. TEM images taken at a concentration of 0.1 mM and hence below the CPC show small cyclic structures with a diameter of ca. 2−4 nm (TEM image A in Figure 3). Above the CPC at 1 mM, no more cyclic structures but adlayers of linear polymer strands with a thickness of ca. 1 nm and a length of more than 20 nm are observed (TEM image B in Figure 3). Similar adlayers were also observed previously on mica surfaces in atomic force microscopy images.[32]

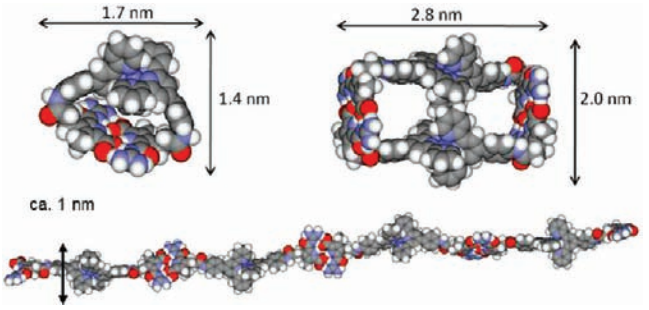

Figure 5. Calculated energy minimized structures of a cyclic dimer, a cyclic tetramer, and the linear polymer along with representative molecular dimensions as obtained from force field calculations.

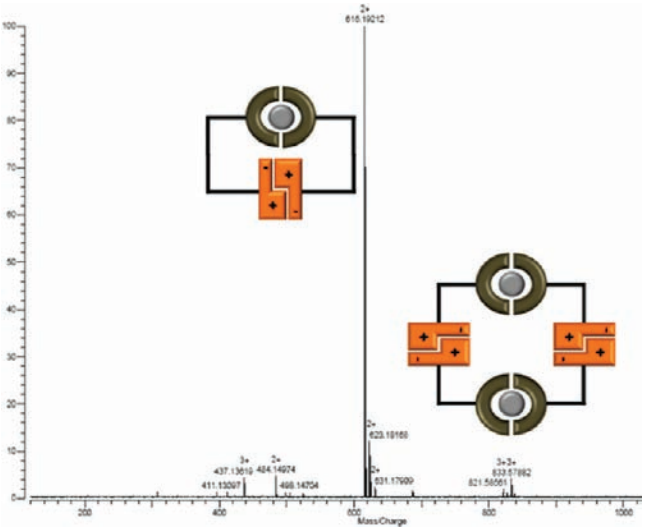

Figure 6. ESI-MS spectrum of **D** (0.2 mM in MeOH) showing a predominant signal for a cyclic dimer and a smaller one for a cyclic tetramer.

To probe the feasibility of the formation of small cycles, we performed molecular modeling studies using the software package Macromodel 8.0 (OPLS force field, GBSA water solvation model). Energy minimized structures (Figure 5) were obtained from a Monte Carlo conformational search with 50.000 steps for each structure. In each case, the resulting minimum was found at least 10 times or more during the simulation. These calculations confirm that the formation of small cycles is geometrically possible in accordance with the TEM images and the postulated ring−chain polymerization mechanism. Furthermore, the calculated molecular dimensions of both the cyclic oligomers as well as the polymer strands are in excellent agreement with the size of the particles observed in the TEM images.

The formation of small cycles in solution was also confirmed by ESI MS (Figure 6). A strong signal for a cyclic dimer at m/z = 616.192 (charge +2) as well as a less intense signal for a tetramer at m/z = 833.578 (charge +3) are observed. However, no signal for a trimer is observed. This is not surprising as only an even number of monomers **1** can form cyclic oligomers. Any odd number of monomers could only form linear oligomers with unsaturated binding sites at each end. The ESI spectra therefore

dx.doi.org/10.1021/ja200941a |*J. Am. Chem. Soc.* 2011, 133, 8961–8971

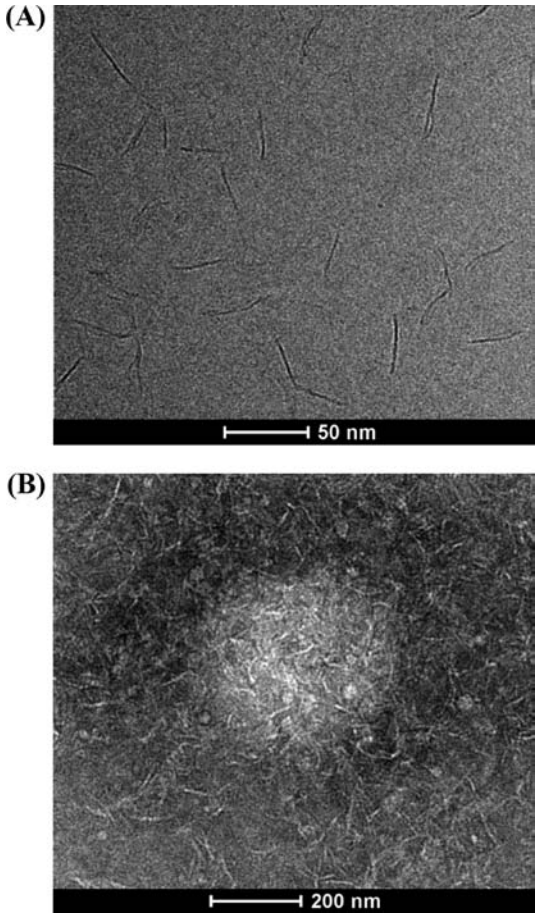

Figure 7. (A) Cryo-TEM image of polymer **D** (c = 0.5 mM in water/DMSO 95/5) showing linear polymer strands. (B) These polymers further assemble into larger densely packed globular aggregates (white sphere in the center) as proven by the negative staining preparation with 1% uranyl acetate. Globules in the diameter range of 200−600 nm can be found.

also suggest the presence of cyclic rather than linear oligomers under dilute conditions.

Cryo-TEM images,[39,40] which provide direct structural data from a vitrified aqueous solutions (c = 0.5 mM in 95:5 water/DMSO), reveal linear semiflexible polymer strands just as well (Figure 7A). The contrast of the data is extraordinarily high due to the presence of iron ions in the aggregates. The estimated thickness of the linear polymers is ca. 1−2 nm (in excellent agreement with the TEM images and the modeling data), and their length on average in water is between 30 and 100 nm. As one monomer has a length of ca. 3.8 nm (according to modeling data), a polymer length of 50 nm translates into an aggregation number of ca. 13 monomers. Furthermore, as seen from a closer inspection of the images, the polymer strands in solution have a tendency to undergo lateral aggregation. For example, in the upper right corner of Figure 7A, two strands can be seen, which aggregate into a double strand. This further aggregation might be explained by hydrophobic interactions between the strands or anion-induced aggregation of the overall positively charged polymers. As the cryo-TEM images were taken from an aqueous solution, it is not surprising that hydrophobic aggregation into larger structures can take place.

To probe for even larger aggregates than just the linear polymers, the complementary use of the negative staining technique was used. Vitrified samples suitable for cryo-TEM are limited with respect to their thickness to ca. 100 nm layers to provide the necessary translucence for the electron beam. Therefore, three-dimensional objects larger than this size range are hardly accessible by this method. After negative staining with 1% uranyl acetate, we could observe a further assembly of the linear polymers into larger globular aggregates with diameters ranging from 200 to 600 nm (Figure 7B). Within the core of these aggregates, the strands are densely packed (these areas are excluded from the stain and therefore appear as white spheres). Toward the globules' outer shell, the strands (still with an apparent thickness of 1−2 nm and a length ranging from 35 to 100 nm) are more loosely arranged. In the areas between the globular aggregates, individual polymer strands can be found as seen in the cryo-TEM images without negative staining salt. Taken all together, the cryo-TEM images therefore demonstrate the formation of linear, semiflexible supramolecular polymers of considerable length even in water and their tendency to further aggregate into larger globular structures.

Light Scattering Studies. To confirm the findings from the electron microscopy studies, we also studied the self-assembly of **1** using dynamic light scattering (DLS) at different concentrations in DMSO (c = 0.5 and 6 mM). As the sample strongly absorbs in the visible wavelength range (due to the colored iron−terpyridine complex), a DLS analysis with typical visible lasers normally used was not possible. We therefore used an IR laser with 831.5 nm wavelength to perform the experiment, as it was shown previously that this allows for the characterization of colored samples by DLS.[41] Measurements were performed at a scattering angle of θ = 90°. Figure 8A displays results for the 0.5 mM solution. Autocorrelation function and decay time distribution clearly show bimodal behavior. One peak corresponds to a hydrodynamic radius in the size range of $r_{H,app}$ = 200−300 nm, and the other corresponds to a hydrodynamic radius above 10 μm. It was not possible to remove these very large aggregates by various attempts to filter the solution. One possibility might be that the large structures are completely destroyed by shear forces during filtration and then re-form in solution afterward, which is perhaps not unexpected for a highly dynamic and reversible self-assembling system. Therefore, long measuring times were chosen to include these very large particles in the measurement (1800 s in the given example). Even though the self-assembled polymer carries charges, the observed bimodal distribution in DLS is not caused by polyelectrolyte effects as evident from the visibility of very strongly scattering large particles in the laser beam by eye. Possibly, the chloride counterions associate with the polymers in DMSO so that the remaining overall charge of the aggregate is not too high. In any case, no polyelectrolyte effects complicate the size analysis by DLS, and it is therefore possible to discuss (apparent) particle sizes. Thereby, it was possible to obtain reproducible results: The bimodal distribution is always detected, and an apparent hydrodynamic radius of r_H = 235 ± 5 nm for the smaller species results. However, as these data result from a measurement at a 90° scattering angle only and no angular extrapolation was performed, the real value likely is somewhat larger. It is reasonable to assume that these particles correspond to similar globular aggregates as seen in the TEM images in water (Figure 7B) even though the DLS data were obtained from DMSO solution and the TEM images from water.

The very high scattering intensity of the large particles (r > 10 μM) does not allow the simultaneous detection of any smaller

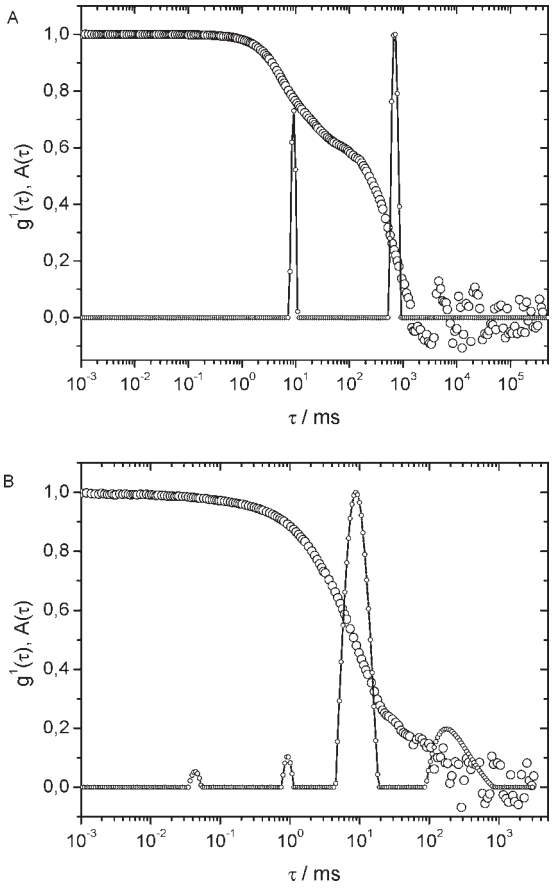

Figure 8. (A) Dynamic light scattering of a solution of **1** in DMSO (c = 0.5 mM). Electric field autocorrelation function $g^1(\tau)$ and distribution of relaxation times $A(\tau)$ (wavelength λ = 831.5 nm, scattering angle θ = 90°). The duration of the measurement was 1800 s. (B) Same experiment at a concentration of 6 mM. Multiple measurements with duration of 5 s each were averaged after excluding runs with a higher intensity caused by very large particles.

species such as individual polymers. Hence, the absence of faster processes indicating small species in this sample does not allow any conclusion whether these particles are not present or can simply not be detected due to the extremely high scattering intensity of the larger particles (scattering intensity scales with r^6). Therefore, to check for smaller species, a concentrated solution (6 mM) was measured multiple times for 5 s, and runs that detected very large particles were disregarded using the software "dust filter". This way, 22 runs were collected and averaged for data analysis. The result is shown in Figure 8B. Different experiments of this kind were performed, differing in accumulation times (5, 10, and 30 s) and in selection criteria for the runs. In all cases, consistently and reproducibly two further species were detected at fast decay times besides the two large species already seen before. The two small species have a hydrodynamic radius of r_H = 1−1.2 nm and 25−35 nm, respectively. For the 1 nm size range, no angular dependence is expected in DLS. Hence, even though the measurements were only taken at one scattering angle (as mentioned above), the data represent a reliable measure for the real size of the particles. The radius of 25−35 nm for the second species again represents only an apparent value, and the real radius might be somewhat larger as no angular extrapolation could be performed.

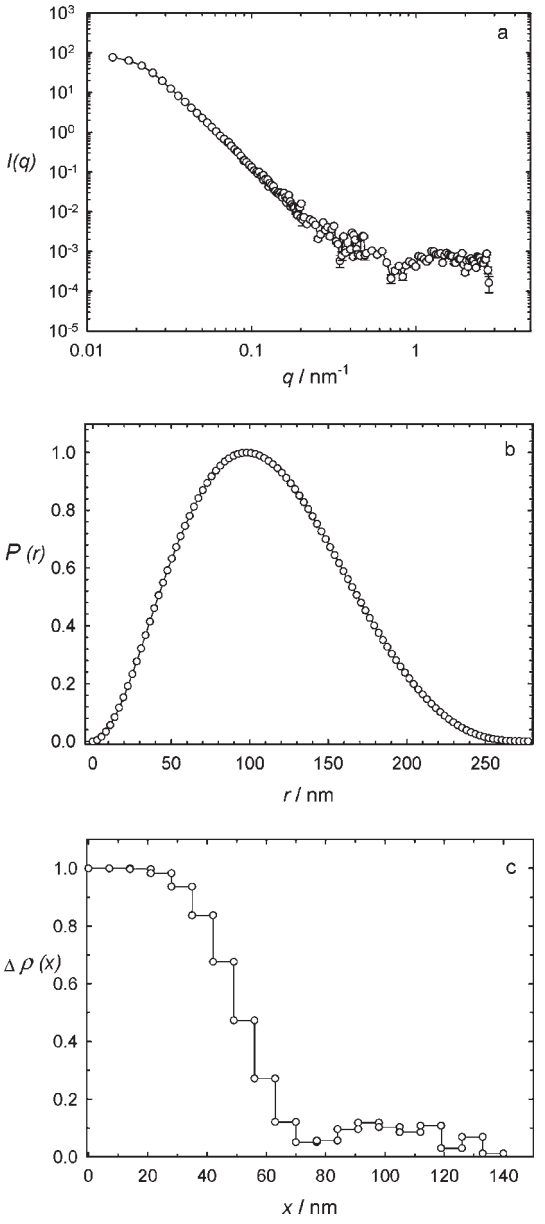

Figure 9. SANS analysis of **1** (2 mM in d_6-DMSO): (a) Scattering curve $I(q)$ (arbitrary units); (b) corresponding pair distance distribution function $P(r)$ indicating particles with a maximum dimension of 265 nm; and (c) corresponding radial density profile $\Delta\rho(x)$ showing a core−shell structure with an inner sphere with higher density and about 60 nm radius and a total radius of about 130 nm.

The DLS measurements therefore further complement the findings obtained from electron microscopy. The small species of ca. 1 nm radius represents the cyclic oligomers (dimers, tetramers, etc.), which were also seen in TEM (Figure 3B) and ESI (Figure 6), confirming also the calculated size of such cycles (Figure 5). The species with an apparent hydrodynamic radius of 25−35 nm are most likely the linear, semiflexible polymer strands seen in TEM and cryo-TEM images. If one assumes stiff linear strands with a diameter of ca. 1−2 nm, one can estimate a polymer length of ca. 240−280 nm from an apparent hydrodynamic radius of 25 nm, corresponding to a polymerization degree of ca. 70 monomers. Of course, the polymers are not completely stiff but semiflexible (as seen in cryo-TEM), so this

dx.doi.org/10.1021/ja200941a |J. Am. Chem. Soc. 2011, 133, 8961–8971

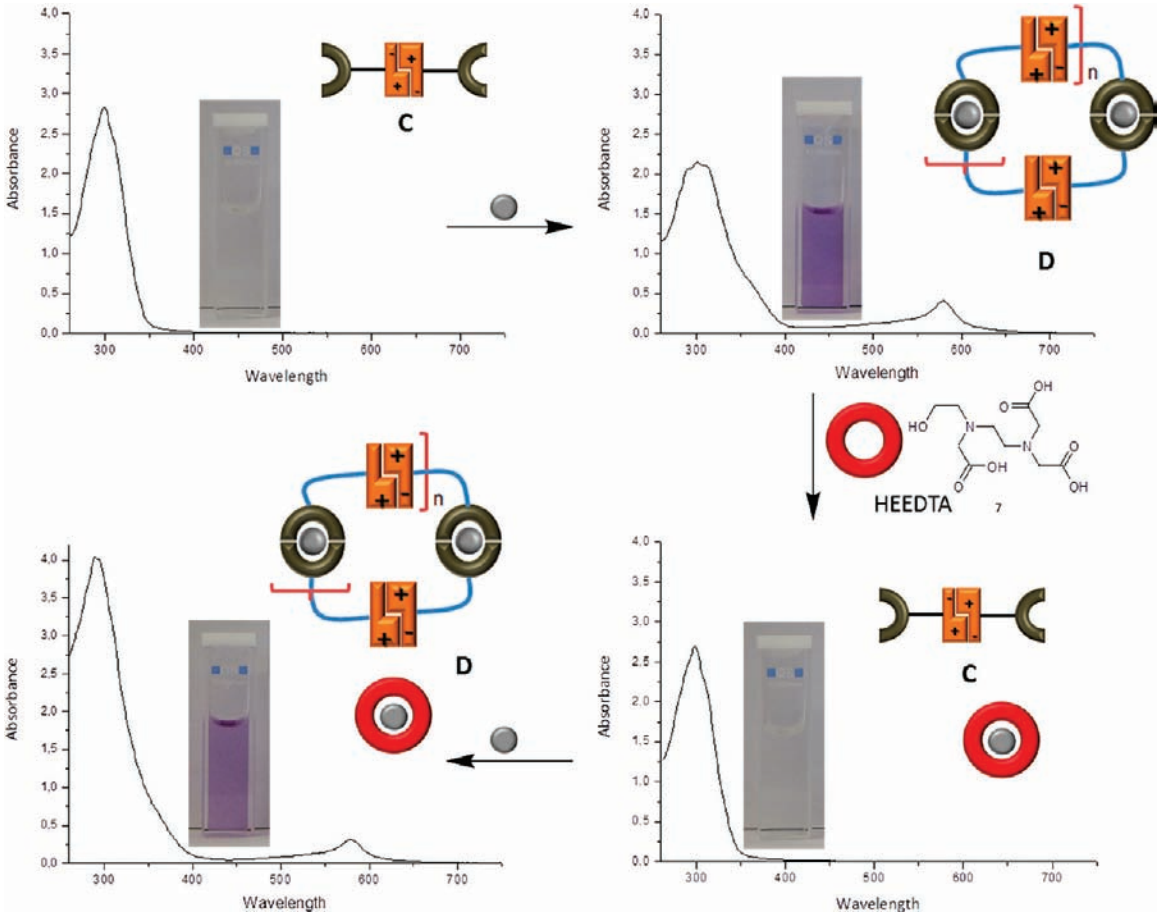

Figure 10. UV−vis complexation studies ([**1**] = 0.06 mM in DMSO). The occurrence of a blue-violet color indicates formation of the metal complex and thus the formation of self-assembled cyclic oligomers **D** from the ion paired dimer **C**. HEEDTA as a competing ligand removes the Fe(II) ions from the terpyridine−metal complex as evident from the decolorization of the sample. Re-addition of excess metal ions then re-forms the cyclic oligomers.

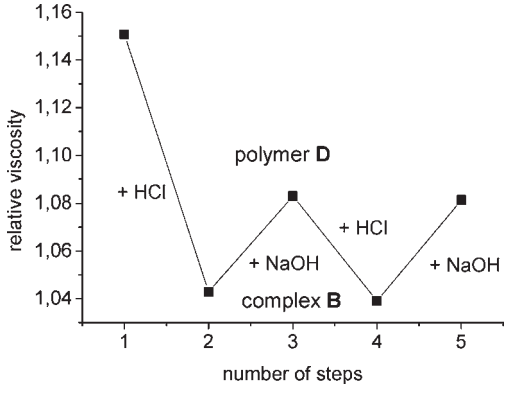

Figure 11. Relative viscosity of a solution of polymer **D** ([**1**] = 6 mM in DMSO) upon stepwise addition of equal amounts of acid or base. Supramolecular polymerization depends on the protonation state of the zwitterion in **1** and can therefore be switched on and off by the addition of acid and base.

number is only an estimate. Nevertheless, a degree of polymerization of this order in DMSO is reasonable. Using the simplified Carothers equation,[42] the degree of polymerization DP for a supramolecular polymer is roughly proportional to $(K_{ass} \cdot C)^{1/2}$, where K_{ass} is the association constant for the intermolecular binding of the monomers and C is the total monomer concentration.[43] At millimolar concentrations, a degree of polymerization of ca. 10^2 requires a stability of the noncovalent interaction, which holds the monomers together of $K_{ass} \geq 10^7$ M^{-1}.[37c] Indeed, both binding interactions, metal−ligand complexation and dimerization of the zwitterion, have an association constant of $K_{ass} \geq 10^8$ in DMSO. The formation of supramolecular polymers of this length from the self-assembly of **1** in DMSO is therefore reasonable.

Small Angle Neutron Scattering. To get further information on the internal structure of the larger particles (the aggregated polymer strands), small angle neutron scattering (SANS) was performed. Samples for SANS were prepared in d_6-DMSO with a concentration of 2.5 g L^{-1} and transferred into optical quality quartz cells with 2 mm path length. SANS studies were performed at the FRM II, Munich, Germany, at the KWS 1 instrument of the Jülich Center for Neutron Science. We used three configurations with the neutron wavelengths λ and sample−detector distances d of λ = 0.45 nm/d = 1.6 m, λ = 0.45 nm/d = 7.6 m, and λ = 1.2 nm/d = 7.6 m. A total scattering vector range of 0.0143 $nm^{-1} < q < 2.8$ nm^{-1} was covered. Data were corrected for empty quartz cell scattering, electronic background, and detector uniformity and were converted to an absolute scale using secondary standards. The data were further corrected by subtracting the contributions from solvent scattering and incoherent background.

dx.doi.org/10.1021/ja200941a |*J. Am. Chem. Soc.* 2011, 133, 8961–8971

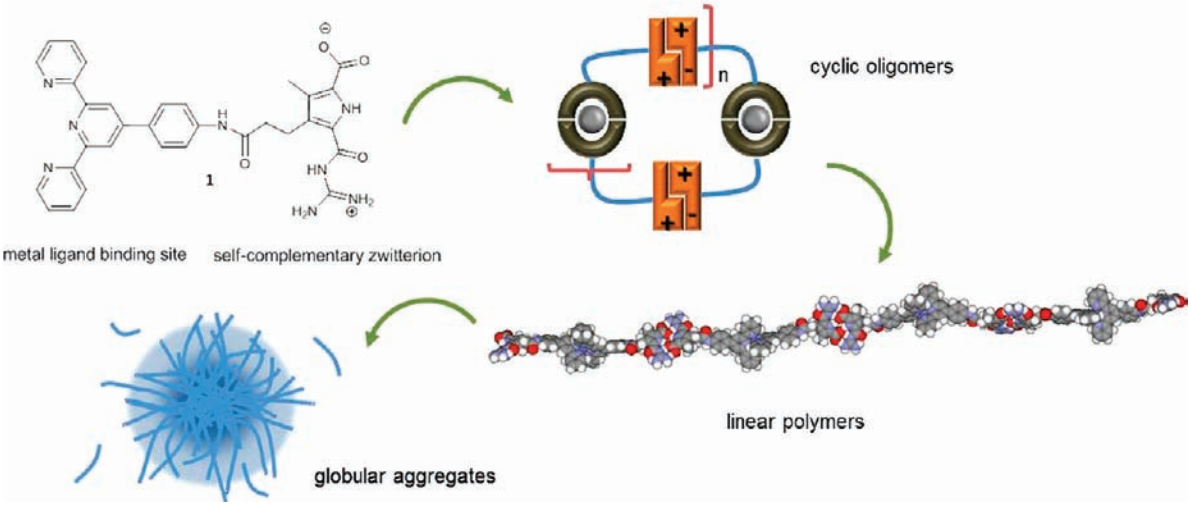

Figure 12. Schematic representation of the self-assembly of monomer **1** in solution.

In the SANS measurement, again large particles with a diameter of >200 nm were detected, confirming the results from the DLS and cryo-TEM measurements. However, SANS now allows one to further probe the internal structure of these aggregates in contrast to DLS. For this purpose, the scattering curve was Fourier transformed into the pair distance distribution function $P(r)$, which basically represents a distance histogram of the particle and thus is dependent on and characteristic for the particle shape and internal density profile.[44] $P(r)$ can be calculated without the need to assume any model in advance from the scattering curve for finite size, randomly oriented particles (or supramolecular assemblies, etc.) in solution. The resulting $P(r)$ is shown in Figure 9b. Most strikingly, the pair distance distribution function $P(r)$ obtained here cannot be described by radially homogeneous particles, even assuming polydispersity. Furthermore, deconvolution into the radial density profile (Figure 9c) shows that the particles consist of a core with a higher density and a less dense shell. This result is consistent with the r_G/r = 0.62 extracted from the SANS measurements prior to the density profile calculation, which is typical of inhomogenous "microgels":[45] A possible origin is a different density or branching profile in the center of the particle as compared to its outer shell. In other words, a denser network type structure is present in the inner region and more "free chains" in the outer region of the particle. This corresponds nicely to the TEM images, which also showed a densely packed core surrounded by a loose shell of polymer particles (Figure 7B). Interestingly, such density profiles are also known for polyelectrolytes that associate with multivalent counterions into larger nanoparticles.[46]

Reversibility of Self-Assembly. As mentioned above, self-assembly of **1** requires both the presence of the metal ion as well as the correct pH range. Therefore, self-assembly can be reversibly switched on and off by adding acid or base to the solution or by removing or adding the metal ion. This reversibility was probed by UV−vis spectroscopy in DMSO (Figure 10). Starting from the blue-violet color of self-assembled cyclic oligomers **D** (c = 0.06 mM in DMSO), addition of an excess of HEEDTA (10 equiv, *N*-(2-Hydroxyethyl)ethylenediaminetriacetic acid) led to complete decomplexation and formation of the ion paired dimers **C** as confirmed by the decolorization of the solution. HEEDTA is a known strong competing ligand system for transition metals like iron(II). It has a significantly higher affinity for Fe(II) than does the terpyridine ligand (log K = 12.3 versus log K = 7, respectively)[47] and therefore quantitatively removes the metal ion from the self-assembled oligomers **D** causing deaggregation into the ion paired dimer **C**. If excess iron(II) is added again, the blue-violet color and the MLCT-band reappear, indicating the reformation of the self-assembled aggregates **D** from the ion paired dimer **C**.

The effect of reversible protonation and deprotonation of the zwitterion in **1** was probed using capillary viscosity studies. The relative viscosity of η = 1.16 of the polymer **D** (DMSO solution, c = 6.8 mM, 25 °C) decreases significantly to η = 1.04 after the addition of aqueous hydrochloric acid (100 μL, 1M) (Figure 11). These values are the same as measured before for the polymer **D** and the metal-complex **B** under these conditions (see also Figure 2). Protonation of the zwitterionic binding site removes its self-complementarity and thus leads to depolymerization. The remaining metal-complexed dimer **B**, however, has a significantly smaller viscosity than does polymer **D**. Upon subsequent addition of the same amount of sodium hydroxide (100 μL, 1 M), the viscosity increases again. The carboxylic acid in **B** is deprotonated, and the self-complementary zwitterion is restored, which immediately dimerizes and thus reforms the polymer **D**. Because of the change of solvent composition (from pure DMSO to aqueous DMSO), the relative viscosity of polymer **D** at this point is smaller than the initial value (η = 1.09 instead of η = 1.16, respectively), reflecting the dependence of the stability of the zwitterionic dimer and hence the degree of polymerization on solvent composition. This external switching between polymer **D** and metal-complex **B** is fully reversible as further additions of acid or base cause again the same changes of the viscosity.

■ CONCLUSION

We have shown here that a small monomer **1** with two orthogonal binding interactions self-assembles into a main-chain supramolecular polymer in polar solvents (DMSO, water). Both binding interactions, the formation of an iron−terpyridine complex and the dimerization of a self-complementary zwitterion, are independent of each other, allowing the system to exist in four different self-aggregated states: a monomer (**A**), a

dx.doi.org/10.1021/ja200941a | *J. Am. Chem. Soc.* 2011, 133, 8961–8971

metal-complexed dimer (**B**) or an ion paired dimer (**C**), and finally either cyclic or linear self-assembled aggregates (**D**). Both binding events can be switched on and off independently from each other (e.g., by removing the metal with a competing ligand and the addition of acid or base) so that reversible external switching between these four states is possible. As both binding interactions are very strong ($K_{ass} \geq 10^8$ in DMSO), self-assembly leads to supramolecular polymers **D** with a significant degree of polymerization already at millimolar concentrations. Because of the flexibility of the molecule, the formation of small cyclic oligomers (e.g., dimers, tetramers, etc.) is also possible, so that the supramolecular polymerization follows a classical ring−chain polymerization model. The semiflexible polymer strands in solution then further aggregate into larger spherical nanostructures of considerable size most likely due to hydrophobic or aromatic stacking interactions between the strands. This stepwise self-assembly process is summarized in Figure 12. All available experimental data (UV/vis spectroscopy, viscosity, TEM, cryo-TEM, DLS, SANS, and molecular modeling) are consistent and fully confirm this model. Hence, the heteroditoic monomer **1** is one of the few systems that forms supramolecular polymers of considerable size even in polar solvents and that can be furthermore switched externally between aggregated and nonaggregated state in two different ways. Such system might be of interest for the development of stimuli responsive materials in the future.

■ ASSOCIATED CONTENT

Supporting Information. Experimental procedure for the synthesis of **1** as well as analytical and spectral characterization data. This material is available free of charge via the Internet at http://pubs.acs.org.

■ AUTHOR INFORMATION

Corresponding Author
franziska.groehn@chemie.uni-erlangen.de; carsten.schmuck@uni-due.de

■ ACKNOWLEDGMENT

Financial support of our work from the DFG and the Fonds of the chemical industry and the Jülich Center for Neutron Science (JCNS) is gratefully acknowledged. We also thank Prof. Christoph Schalley and Henrik Winkler (FU Berlin, Germany) for measuring the ESI-MS spectrum, Wilhelm Sicking (University of Duisburg-Essen) for help with the molecular modeling calculations, and Dr. Henrich Frielinghaus (JCNS, Germany) for help with the SANS measurements.

■ REFERENCES

(1) For selected reviews on supramolecular polymers, see: (a) Brunsveld, B. J. B.; Folmer, E. W.; Meijer, E. W.; Sijbesma, R. P. *Chem. Rev.* **2001**, *101*, 4071–4097. (b) Bouteiller, L. *Adv. Polym. Sci.* **2007**, *207*, 79–112. (c) Binder, W. H.; Zirbs, R. *Adv. Polym. Sci.* **2007**, *207*, 1–78. (d) Rieth, S.; Baddeley, C.; Badjic, J. D. *Soft Matter* **2007**, *3*, 137–154. (e) Armstrong, G.; Buggy, M. *J. Mater. Sci.* **2005**, *40*, 547–559. (f) Ciferri, A. *Supramolecular Polymers*; Taylor & Francis: Boca Raton, Florida, 2005. (g) Sherrington, D. C.; Taskinen, K. A. *Chem. Soc. Rev.* **2001**, *30*, 83–93.

(2) (a) Pollino, J. M.; Weck, M. *Chem. Soc. Rev.* **2005**, *34*, 193–207. (b) Rotello, V.; Thayumanavan, S. *Molecular Recognition and Polymers*; Wiley: New York, 2008.

(3) (a) Fox, J. D.; Rowan, S. J. *Macromolecules* **2009**, *42*, 6823–6835. (b) Shimizu, L. S. *Polym. Int.* **2007**, *56*, 444–452. (c) Kyung Yang, A.; Ambade, A. V.; Weck, M. *Chem. Soc. Rev.* **2011**, *40*, 129–137.

(4) (a) Schneider, H.-J. *Angew. Chem., Int. Ed.* **2009**, *48*, 3924–3977. (b) Williams, D. H.; Westwell, M. S. *Chem. Soc. Rev.* **1998**, *27*, 57–64. (c) Bissantz, C.; Kuhn, B.; Stahl, M. *J. Med. Chem.* **2010**, *53*, 5061–5084.

(5) Serpe, M. J.; Craig, S. L. *Langmuir* **2007**, *23*, 1626–1634.

(6) (a) de Greef, T. F. A.; Meijer, E. W. *Nature* **2008**, *453*, 171–173. (b) Bosman, A. W.; Brunsveld, L.; Folmer, B. J. B.; Sijbesma, R. P.; Meijer, E. W. *Macromol. Symp.* **2003**, *201*, 143–154.

(7) Cordier, P.; Tournilhac, F.; Soulié-Ziakovic, C.; Leibler, L. *Nature* **2008**, *451*, 977–980.

(8) (a) Lehn, J.-M. *Polym. Int.* **2002**, *51*, 825–839. (b) Berl, V.; Schmutz, M.; Krische, M. J.; Khoury, R. G.; Lehn, J.-M. *Chem.-Eur. J.* **2002**, *8*, 1227–1244. (c) Kotera, M.; Lehn, J.-M.; Vigneron, J.-P. *J. Chem. Soc., Chem. Commun.* **1994**, 197–199. (d) Gulik-Krczywicki, T.; Fouquey, C.; Lehn, J.-M. *Proc. Natl. Acad. Sci. U.S.A.* **1993**, *90*, 163–167.

(9) (a) Sijbesma, R. P.; Beijer, F. H.; Brunsveld, L.; Folmer, B. J. B.; Hirschberg, J. H. K. K.; Lange, R. F.; Lowe, J. K. L.; Meijer, E. W. *Science* **1997**, *278*, 1601–1604. (b) Folmer, B. J. B.; Sijbesma, R. P.; Versteegen, R. M.; van der Rijt, J. A. J.; Meijer, E. W. *Adv. Mater.* **2000**, *12*, 874–878.

(10) (a) Beijer, F. H.; Sijbesma, R. P.; Kooijman, H.; Spek, A. L.; Meijer, E. W. *J. Am. Chem. Soc.* **1998**, *120*, 6761–6769. (b) Söntjens, S. M. H.; Sijbesma, R. P.; van Genderen, M. H. P.; Meijer, E. W. *J. Am. Chem. Soc.* **2000**, *122*, 7487–7493.

(11) (a) Schmuck, C.; Wienand, W. *Angew. Chem., Int. Ed.* **2001**, *40*, 4363–4369. (b) Zimmerman, S. C.; Corbin, P. S. *Struct. Bonding* **2000**, *96*, 63–94.

(12) (a) Jeffrey, G. A. *An Introduction to Hydrogen Bonding*; Oxford University Press: New York, 1997. (b) Hunter, C. A. *Angew. Chem., Int. Ed.* **2004**, *43*, 5310–5324.

(13) (a) Rehm, T.; Schmuck, C. *Chem. Commun.* **2008**, 801–813. (b) Oshovsky, G. V.; Reinhoudt, D. N.; Verboom, W. V. *Angew. Chem., Int. Ed.* **2007**, *46*, 2366–2393. (c) Zayed, J.; Nouvel, N.; Rauwald, U.; Scherman, O. A. *Chem. Soc. Rev.* **2010**, *39*, 2806–2816.

(14) (a) Obert, E.; Bellot, M.; Bouteiller, L.; Andrioletti, F.; Lehen-Ferrenbach, C.; Boué, F. *J. Am. Chem. Soc.* **2007**, *129*, 15601–15605. (b) Yoshikawa, I.; Sawayama, J.; Araki, K. *Angew. Chem., Int. Ed.* **2008**, *47*, 1038–1041. (c) Merschky, M.; Wyszogrodzka, M.; Haag, R.; Schmuck, C. *Chem.-Eur. J.* **2010**, *16*, 14242–14246. (d) Mes, T.; Smulders, M. M. J.; Palmans, A. R. A.; Meijer, E. W. *Macromolecules* **2010**, *43*, 1981–1991.

(15) However, ethylene glycol only exhibits a stabilizing effect as compared to aqueous solvents (as in ref 14c). In less polar solvents, it destabilizes H-bonded systems due to competitive intramolecular H-bonding: (a) de Greef, T. F. A.; Nieuwenhuizen, M. M. L.; Stals, P. J. M.; Fitie, C. F. C.; Palmans, A. R. A.; Sijbesma, R. P.; Meijer, E. W. *Chem. Commun.* **2008**, 4306–4308. (b) de Greef, T. F. A.; Nieuwenhuizen, M. M.; Sijbesma, R. P.; Meijer, E. W. *J. Org. Chem.* **2010**, *75*, 598–610.

(16) (a) Rehm, T.; Schmuck, C. *Chem. Soc. Rev.* **2010**, *39*, 3597–3611. (b) Gröhn, F. *Soft Matter* **2010**, *6*, 4296–4302.

(17) Ryu, J.-H.; Hong, D.-J.; Lee, M. *Chem. Commun.* **2008**, 1043–1054.

(18) (a) Neelakandan, P. P.; Pan, Z.-Z.; Hariharan, M.; Zheng, Y.; Weissman, H.; Rybtchinski, B.; Lewis, F. D. *J. Am. Chem. Soc.* **2010**, *132*, 15808–15813. (b) Krieg, E.; Shirman, E.; Weissman, H.; Shimoni, E.; Wolf, S. G.; Pinkas, I.; Rybtchinski, B. *J. Am. Chem. Soc.* **2009**, *131*, 14365–14373. (c) Kaiser, T.; Wang, H.; Stepanenko, V.; Würthner, F. *Angew. Chem., Int. Ed.* **2007**, *46*, 5541–5544. (d) Zhang, X.; Rehm, S.; Safont-Sempere, M. M.; Würthner, F. *Nat. Chem.* **2009**, *1*, 623–629.

(19) Würthner, F. *Chem. Commun.* **2004**, 1564–1579.

(20) (a) Garcia, F.; Sanchez, L. *Chem.-Eur. J.* **2010**, *16*, 3138–3146. (b) Yagai, S.; Kubota, S.; Saito, H.; Unoike, K.; Karatsu, T.; Kitamura, A.; Ajayaghosh, A.; Kanesato, M.; Kikkawa, Y. *J. Am. Chem. Soc.* **2009**, *131*, 5408–5410. (c) Garcia, F.; Aparicio, F.; Marenchino, M.; Campos-Olivas, R.; Sanchez, L. *Org. Lett.* **2010**, *12*, 4264–4267.

(21) Percec, V.; Imam, M. R.; Peterca, M.; Wilson, D. A.; Heiney, P. A. *J. Am. Chem. Soc.* **2009**, *131*, 1294–1304.
(22) Yin, M.; Shen, J.; Pisula, W.; Liang, M.; Zhi, L.; Müllen, K. *J. Am. Chem. Soc.* **2009**, *131*, 14618–14619.
(23) (a) Schmidt, R.; Uemura, S.; Würthner, F. *Chem.-Eur. J.* **2010**, *16*, 13706–13715. (b) Yagai, S.; Kinoshita, T.; Higashi, M.; Kishikawa, K.; Nakanishi, T.; Karatsu, T.; Kitamura, A. *J. Am. Chem. Soc.* **2007**, *129*, 13277–13287. (c) Yagai, S.; Higashi, M.; Karatsu, T.; Kitamura, A. *Chem. Mater.* **2005**, *17*, 4392–4398. (d) Chen, Z.; Lohr, A.; Saha-Möller, C. R.; Würthner, F. *Chem. Soc. Rev.* **2009**, *38*, 564–584.
(24) (a) Harada, A.; Takashima, Y.; Yamaguchi, H. *Chem. Soc. Rev.* **2009**, *38*, 875–882. (b) Becherer, M. S.; Schade, B.; Böttcher, C.; Hirsch, A. *Chem.-Eur. J.* **2009**, *15*, 1637–1648. (c) Koopmans, C.; Ritter, H. *J. Am. Chem. Soc.* **2007**, *129*, 3502–3503. (d) Kretschmann, O.; Steffens, C.; Ritter, H. *Angew. Chem., Int. Ed.* **2007**, *46*, 2708–2711.
(25) (a) Reinhold, F.; Kolb, U.; Lieberwirth, I.; Gröhn, F. *Langmuir* **2009**, *25*, 1345–1351. (b) Li, Y.; Yildiz, H. U.; Müllen, K.; Gröhn, F. *Biomacromolecules* **2009**, *10*, 530–540.
(26) For some recent reviews on metallo-supramolecular polymers, see: (a) Dobrawa, R.; Würthner, F. *J. Polym. Sci., Part A: Polym. Chem.* **2005**, *43*, 4981–4995. (b) Hofmeier, H.; Schubert, U. S. *Chem. Soc. Rev.* **2004**, *33*, 373–399. (c) Chiper, M.; Hoogenboom, R.; Schubert, U. S. *Macromol. Rapid Commun.* **2009**, *30*, 565–578. (c) Shunmugam, R.; Gabriel, G. J.; Khaled, A. A.; Tew, G. N. *Macromol. Rapid Commun.* **2010**, *31*, 784–793. (d) Schubert, U. S.; Newkome, G. R.; Maners, I. . ACS Symposium Series 928, 2006. (e) Friese, V. A.; Kurth, D. G. *Curr. Opin. Colloid Interface Sci.* **2009**, *14*, 81–93.
(27) (a) Gröhn, F.; Klein, K.; Brand, S. *Chem.-Eur. J.* **2008**, *14*, 6866–6869. (b) Willerich, I.; Gröhn, F. *Chem.-Eur. J.* **2008**, *14*, 9112–9116. (c) Gröhn, F. *Macromol. Chem. Phys.* **2008**, *209*, 2295–2301. (d) Willerich, I.; Ritter, H.; Gröhn, F. *J. Phys. Chem. B* **2009**, *113*, 3339–3354. (e) Gröhn, F.; Klein, K.; Koynov, K. *Macromol. Rapid Commun.* **2010**, *31*, 75–80.
(28) (a) Hofmeier, H.; Schubert, U. S. *Chem. Commun.* **2005**, 2423–2432. (b) Schmittel, M.; Mahata, K. *Angew. Chem., Int. Ed.* **2008**, *47*, 5284–5286.
(29) (a) Hofmeier, H.; El-ghayoury, A.; Schenning, A. P. H. J.; Schubert, U. S. *Chem. Commun.* **2004**, 318–319. (b) Hofmeier, H.; Hoogenboom, R.; Wouters, M. E. L.; Schubert, U. S. *J. Am. Chem. Soc.* **2005**, *127*, 2913–2921.
(30) (a) Furusho, Y.; Yashima, E. *Macromol. Rapid Commun.* **2011**, *32*, 136–146. (b) Yashima, E.; Maeda, K.; Iida, H.; Furusho, Y.; Nagai, K. *Chem. Rev.* **2009**, *109*, 6102–6211. (c) Yashima, E.; Maeda, K.; Furusho, Y. *Acc. Chem. Res.* **2008**, *41*, 1166–1180.
(31) Some recent examples and reviews on switchable nanoassemblies: (a) Voskuhl, J.; Fenske, T.; Stuart, M. C. A.; Wibbeling, B.; Schmuck, C.; Ravoo, B. J. *Chem.-Eur. J.* **2010**, *16*, 8300–8306. (b) Rodler, F.; Linders, J.; Fenske, T.; Rehm, T.; Mayer, C.; Schmuck, C. *Angew. Chem., Int. Ed.* **2010**, *49*, 8747–8750. (c) Du, J.; Tang, Y.; Lewis, A. L.; Armes, S. P. *J. Am. Chem. Soc.* **2005**, *127*, 17982–17983. (d) Versluis, F.; Tomatsu, I.; Kehr, S.; Fregonese, C.; Tepper, A. W. J. W.; Stuart, M. C. A.; Ravoo, B. J.; Koning, R. I.; Kros, A. *J. Am. Chem. Soc.* **2009**, *131*, 13186–13187. (e) Ghosh, S.; Reches, M.; Gazit, E.; Verma, S. *Angew. Chem., Int. Ed.* **2007**, *46*, 2002. (f) Menand, M.; Jabin, I. *Chem.-Eur. J.* **2010**, *16*, 2159–2169. (g) Leung, K. C.-F.; Chak, C.-P.; Lo, C.-M.; Wong, W.-Y.; Xuan, S.; Cheng, C. H. K. *Chem. Asian J.* **2009**, *4*, 364–381. (h) Rowan, S. J. *Polym. Prepr.* **2009**, *50*, 339–340. (i) Beck, J. B.; Rowan, S. J. *J. Am. Chem. Soc.* **2003**, *125*, 13922–13923. (j) Wang, C.; Guo, Y.; Wang, Z.; Zhang, X. *Langmuir* **2010**, *26*, 14509–14511. (k) Wang, F.; Zhang, J.; Ding, X.; Dong, S.; Liu, M.; Zheng, B.; Li, S.; Wu, L.; Yu, Y.; Gibson, H. W. *Angew. Chem., Int. Ed.* **2010**, *49*, 1090–1094. (l) Yagai, S.; Kitamura, A. *Chem. Soc. Rev.* **2008**, *37*, 1520–1529. (m) Willerich, I.; Gröhn, F. *Angew. Chem., Int. Ed.* **2010**, *49*, 8104–8108.
(32) Gröger, G.; Stepanenko, V.; Würthner, F.; Schmuck, C. *Chem. Commun.* **2009**, 698–700.
(33) Schmuck, C.; Wienand, W. *J. Am. Chem. Soc.* **2003**, *125*, 452–459.
(34) Mutai, T.; Cheon, J. D.; Arita, S.; Araki, K. *J. Chem. Soc., Perkin Trans. 2* **2001**, *7*, 1045–1050.
(35) Schmuck, C. *Eur. J. Org. Chem.* **1999**, 2397–2403.
(36) Hofmeier, H.; Schubert, U. S. *Chem. Commun.* **2004**, 373–399.
(37) (a) Ciferri, A. *Macromol. Rapid Commun.* **2002**, *23*, 511–529. (b) de Greef, T. F. A.; Smudlers, M. M. J.; Wolffs, M.; Schenning, A. P. H. J.; Sijbesma, R. P.; Meijer, E. W. *Chem. Rev.* **2009**, *109*, 5687–5754. (c) ten Cate, A. T.; Sijbesma, R. P. *Macromol. Rapid Commun.* **2002**, *23*, 1094–1112.
(38) (a) Hagy, M. C.; Chen, C.-C.; Dormidontova, E. E. *Macromolecules* **2007**, *40*, 3408–3421. (b) Ercolani, G.; Mandolini, L.; Mencarelli, P.; Roelens, S. *J. Am. Chem. Soc.* **1993**, *115*, 3901–3908. (c) Chen, C.-C.; Dormidontova, E. E. *Macromolecules* **2004**, *37*, 3905–3917. (d) Ercolani, G.; Di Stefano, S. *J. Phys. Chem. B* **2008**, *112*, 4662–4665.
(39) (a) Dubochet, J.; McDowall, A. W. *J. Microsc. (Oxford, U.K.)* **1981**, *124*, Rp3–Rp4. (b) Dubochet, J.; Chang, J. J.; Freeman, R.; Lepault, J.; McDowall, A. W. *Ultramicroscopy* **1982**, *10*, 55–61. (c) Dubochet, J.; Lepault, J.; Freeman, R.; Berriman, J. A.; Homo, J. C. *J. Microsc. (Oxford, U.K.)* **1982**, *128*, 219–237.
(40) For a recent review, see: Friedrich, H.; Frederik, P. M.; de With, G.; Sommerdijk, N. A. J. M. *Angew. Chem., Int. Ed.* **2010**, *49*, 7850–7858.
(41) Ruthard, C.; Maskos, M.; Kolb, U.; Gröhn, F. *Macromolecules* **2009**, *42*, 830–840.
(42) Martin, R. B. *Chem. Rev.* **1996**, *96*, 3043–3064.
(43) The Carothers equation is based on an isodesmic growth mode (also called equal K model). However, for a high concentration of monomers well above the CPC, the degrees of polymerization for an isodesmic and a ring−chain polymerization are equal. Hence, as a first approximation, the use of the Carothers equation is surely justified here.
(44) (a) Glatter, O. *Acta Phys. Austriaca* **1977**, *47*, 83–102. (b) Glatter, O. *J. Appl. Crystallogr.* **1977**, *10*, 415–421. (c) Glatter, O. *J. Appl. Crystallogr.* **1980**, *13*, 577–584. (d) Gröhn, F.; Bauer, B. J.; Amis, E. J. *Macromolecules* **2001**, *34*, 6701–6707.
(45) Kunz, D.; Thurn-Albrecht, T.; Burchard, W. *Colloid Polym. Sci.* **1983**, *261*, 635–646.
(46) Yildiz, U. H.; Koynov, K.; Gröhn, F. *Macromol. Chem. Phys.* **2009**, *210*, 1678–1690.
(47) Martell, A. E.; Smith, R. M. *Critical Stability Constants*; Plenum Press: New York, 1974.